CONF-8810155--18

CONF-8810155--18

DE89 002983

ANALYSIS OF THE THERMAL RESPONSE OF A BWR MARK-I CONTAINMENT SHELL TO DIRECT CONTACT BY MOLTEN CORE MATERIALS

T. S. Kress and J. C. Cleveland
Oak Ridge National Laboratory
Oak Ridge, Tennessee 37831

For presentation at
16th Water Reactor Safety Information Meeting
October 27, 1988

ANALYSIS OF THE THERMAL RESPONSE OF A BWR MARK-I CONTAINMENT SHELL TO DIRECT CONTACT BY MOLTEN CORE MATERIALS*

T. S. Kress and J. C. Cleveland
Oak Ridge National Laboratory
Oak Ridge, Tennessee 37831

ABSTRACT

This study was undertaken to evaluate the thermal response of a BWR Mark-I containment shell in the event of an accident severe enough for molten core materials to fall into the cavity beneath the reactor vessel and eventually come into direct contact with the shell. An existing ORNL three-dimensional transient heat transport computer code, HEATING-6, was used for a specific 2-D case (and variations) for which representative melt/shell boundary conditions required as input were available from other studies.

In addition to the use of HEATING-6, a simplified analytical steady-state correlation was developed and given the name BWR Liner Analysis Program (BWRLAP). BWRLAP was "benchmarked" by comparison with HEATING-6 and was then used to make a number of parametric calculations to investigate the sensitivities of the results to the inputs.

INTRODUCTION

A mode of early containment failure for BWR Mark-I systems has been identified to result from heating of the containment steel shell by the direct contact of molten core materials (Ref. 1). The issue in question is whether or not the shell would actually fail as a result of this contact. The present study was undertaken to develop a means to evaluate the thermal response of the shell for initial and boundary conditions at contact that are predicted by other studies that use melt progression (MP) and molten core concrete interaction (MCCI) codes.

The geometric aspects of the problem are illustrated in Figure 1 which is a diagram of our representation of the Peach Bottom system (although Figure 1 treats the shell as being vertical for computational convenience, it is actually imbedded in the floor at a 45° angle). Above the floor level, there is an air gap between the back side of the shell and the surrounding concrete. Below the floor level, this gap is filled with sand (there are plant-specific differences in these details).

---

*Research sponsored by the Office of Nuclear Regulatory Research, U.S. Nuclear Regulatory Commission under Interagency Agreement DOE 0551-0551-A1 with the U.S. Department of Energy under contract DE-AC05-84OR21400 with the Martin Marietta Energy Systems, Inc.

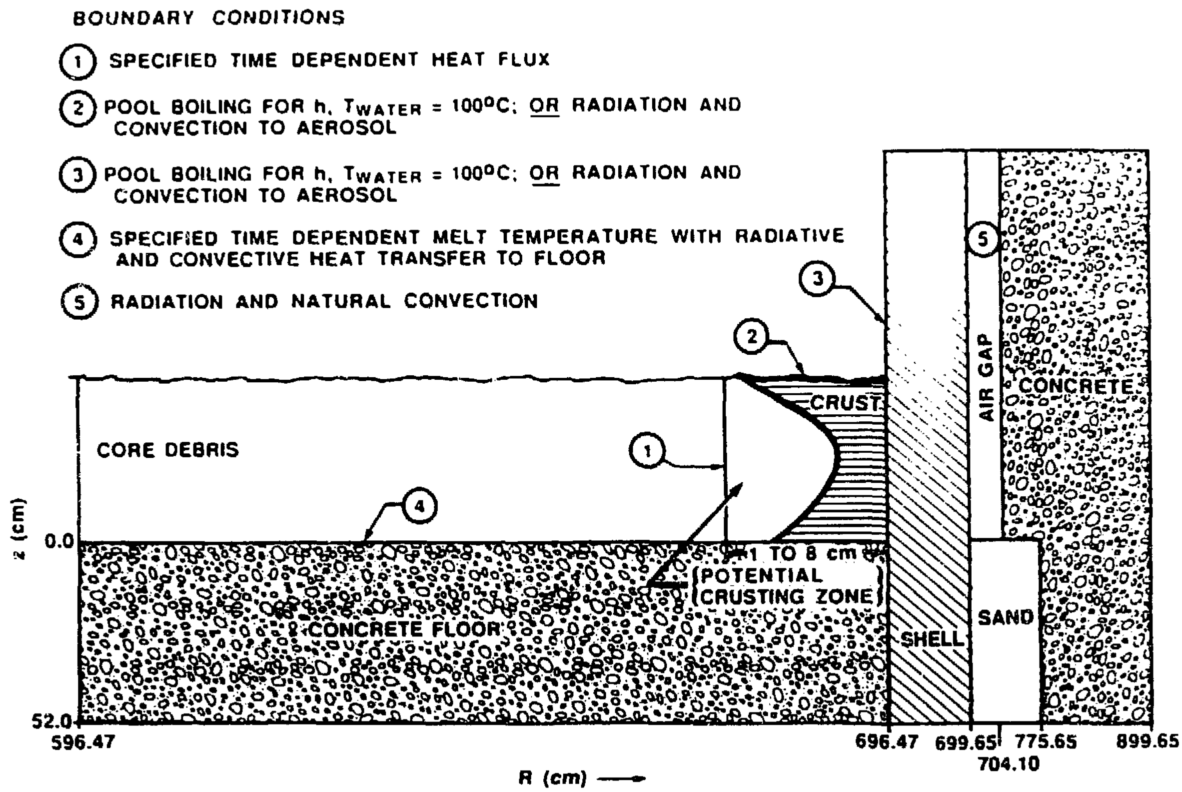

Fig. 1. Mark-1 Containment shell model for heatup analysis.

Our qualitative view of what occurs when the melt contacts the shell is that the interface between the melt and the shell immediately acquires the classical "perfect contact" interfacial temperature given by:

$$T_i = \frac{T_m + T_s[(kdC_p)_s/(kdC_p)_m]^{1/2}}{1 + [(kdC_p)_s/(kdC_p)_m]^{1/2}} .$$

Under essentially all circumstances of interest to this issue, this interfacial temperature will be well below the melt solidification temperature, and, therefore, it would be expected that a crust would quickly form at the melt/shell interface and would begin to grow in thickness as the thermal wave moves backward into the melt. If there is water overlying the melt, this crust growth would be enhanced by heat transfer from the crust top surface to the boiling water. The water would also cool the region of the shell just above the melt/crust providing a sink for the heat transferred through the crust to the shell. Heat will also be transferred from the backside of the shell in the region of the air gap via radiation and natural convection to the surrounding concrete. Below the floor level, heat will be conducted from the shell through the sand into the concrete. Heat will also be transferred downward from the melt into the concrete floor. Any crust that is formed could exhibit a dynamic behavior — first growing and then shrinking again as the shell undergoes its transient heat-up. If the melt conditions are constant, an equilibrium crust thickness could be attained.

The concrete behind the shell would serve as a large heat capacitance to absorb energy as it slowly heats up. The thermal response of the shell is rapid compared to the concrete thermal response. For constant melt conditions, a quasi-equilibrium state will likely be achieved in which the shell arrives at a quasi-steady temperature distribution. The major heat sink prior to the quasi-steady condition would be the water cooling the shell above the melt (or, if water is not present, convective and radiative heat transfer into the drywell atmosphere). The melt itself is expected to decrease in temperature with time, perhaps allowing the shell temperature to reach a maximum (if failure does not occur) and subsequently to decrease as the melt cools.

The above qualitative description implies that the shell essentially stays in place at its original location. It is likely that the shell will fail if its temperature approaches 1000 K. Stress analyses are needed to confirm this supposition.

APPROACH

The Heating-6 Model

To address this issue, we used an existing ORNL three-dimensional transient heat transport computer program called HEATING-6. This code uses finite difference techniques to solve the general heat conduction equation with internal heat generation. With HEATING-6, the "volume" to be modeled can be divided into any number of arbitrary regions each of which can have its own individual thermal properties as functions of both time and temperature. The boundaries between regions and between internal nodes can be connected to each other by conduction or by radiation and convection to simulate an air gap. Phase changes can be simulated by temporarily specifying properties in such a way that a node will absorb a given amount of energy (the latent heat) with small increase in temperature. After the phase change, the node properties can be internally re-specified to represent the new phase.

Options for boundary nodes include specification of: temperatures that can be functions of time, radiative heat transfer to any sink (which can also have a specified time variable temperature), convective heat transfer with a specified heat transfer coefficient that can be either an arbitrary function of time or some specified function of the average of the boundary temperature and the sink temperature. Alternatively, the code will allow the specification of a time-variable heat flux across any boundary. The HEATING-6 code is fully documented (Ref. 2), has undergone all ORNL quality assurance requirements, and has been extensively verified (Refs. 3, 4, and 5).

The melt/shell region of the Mark I drywell was modelled with HEATING-6 using R-Z geometry as shown in Figure 1. To simplify the noding procedure, the shell was treated as being vertical and the melt depth was increased to a value equal to the full contact distance (i.e., the slant height).

Moving boundaries are not explicitly modeled in HEATING-6. Consequently, to simulate the dynamic crust behavior, the following procedure was used. A potential crusting region was initially defined having a size selected to be slightly larger than the expected real maximum crust thickness (iteration on this was necessary). The heat flux at the melt/crust interface [determined in our study by the prior use of CORCON as given by $h_m(T_m - T_c)$] was specified as input into the face of the potential crusting region. The crust region was given property specifications such that, for temperatures at or below T_c (the "crusting temperature"), the nodes would have thermal properties representative of the solidified melt. Nodes in the potential crusting region with temperatures above the crusting temperature were specified to have an arbitrarily high thermal conductivity and a low specific heat.

The practical effect of this procedure is the same as if there were a crust with a moving interface that is heated by convective transfer from a melt region so long as the specific heat of the "melt" portion of the potential crusting region is low enough that the stored energy change is negligible compared to the through-put heat flux.

The crust region is allowed to have internal volumetric heat generation that is input as a function of time. This input is also obtained from the MCCI code and can be specified to represent any combination of the decay heat and the chemical energy generated as a result of the melt-concrete interaction. Heat transfer out of the crust is by conduction into the shell, into the concrete floor, and into the overlying water undergoing pool boiling. For this boiling heat transfer, the full flat plate pool-boiling curve is used in which the temperature difference between the crust and the water determines the heat flux as well as whether or not the boiling regime is nucleate or film. The same pool boiling relationship is also used to determine the direct contact cooling of the shell by the water pool.

The heat flux from the melt region downward into the concrete floor as determined by CORCON is also an input parameter.

The heat-loss from the exterior side of the shell across the air gap to the concrete is specified to be natural convection plus radiation. In order to close the problem, an adiabatic boundary is placed at a sufficiently large distance around the modelled region.

As the HEATING-6 code does not recognize possible failure and movement of the shell due to reduced strength at high temperatures, our model allows the temperature of any node in the shell to increase to its melting point and absorb the phase change energy at essentially constant temperature. The material in the node is then assumed to be instantaneously replaced with the pseudo-melt material of the potential crusting region. This material is allowed to subsequently freeze into an internal crust if so dictated by the subsequent heat transfer and temperatures.

The BWRLAP Model

Because of the modeling complexity, the time required (for example, 2 CPU hours on the IBM 3033 computer), and the expense, it is sometimes difficult to use an extensive code such as HEATING-6 for the large number of cases that would be needed to fully examine the sensitivity of the results to the input parameters. Consequently, to develop insight into the issue, provide guidance for running HEATING-6, and to investigate the sensitivity of the results to the assumptions and the input values, a simplified (but qualitatively and quantitatively representative) correlational model was developed for application on a PC and given the name BWR Liner Analysis Program (BWRLAP). A detailed description and derivation of BWRLAP is presented in Appendix I. BWRLAP calculates the shell maximum temperature for an assumed quasi-steady state condition as discussed in the introduction. The shell is treated as a fin with heat input along its length by convection from the melt to the crust interface and series conduction in the crust to the shell. BWRLAP allows heat to be lost from the exterior side of the shell by radiation and natural convection to the concrete and by conduction along its length to its interface with the water pool. Heat losses from the crust to the water and to the concrete floor are accounted for by benchmarking the correlation with the HEATING-6 results.

The BWRLAP model should not be viewed as a solution to the 2-D conduction problem but, rather, as a correlational algorithm for the HEATING-6 results. There are essentially two effects of the crust that must be accounted for:

1. The crust allows some fraction of the heat it receives from the melt to be lost off its top and bottom surfaces and to not be delivered to the shell directly.

2. Because of the 2-D nature of the heat transport through the crust, some of the heat is "shunted" upward and enters the shell at a higher position. For a given total transfer of heat into the shell, this will have the effect of lowering the maximum shell temperature.

BWRLAP accounts for both of these effects by utilizing a semi-mechanistic heat transfer algorithm for the heat passing from the melt and through the crust into the shell at each elevation (see Appendix I). Consequently, the BWRLAP correlation must be benchmarked directly to the "true" HEATING-6 results. To accomplish this benchmarking, the following expedient is used. An effective melt depth is used in the BWRLAP model that consists of the actual depth divided by the product of cos 45° (to correct for the slant height) and a correlating parameter that is greater than 1.0. The product is called an "effectiveness factor" (EF).

RESULTS OF CALCULATIONS

HEATING-6 Cases

Five cases were run with the HEATING-6 model, and results are reported here. The input for the first three cases primarily came from early results of the ORNL BWRSAT Programs' application of MP and MCCI codes. The other two cases were designed to benchmark BWRLAP.

CASE-1:

This case is designated as the "base" case to be consistent with the designation given to it by the BWRSAT staff who used their state-of-the-art code called BWRSAR to calculate the melt conditions upon exiting the reactor vessel and then creatively used CORCON (by a method described in a companion paper in these proceedings) to determine the conditions of the melt as it spreads out over the cavity floor and interacts with the concrete. An important feature of this case is that, in the use of BWRSAR, the core materials were arbitrarily held in place inside the reactor vessel until substantial quantities (75%) were molten and at a high temperature. High limestone concrete was assumed for these CORCON calculations. Input for HEATING-6 for this case and subsequent cases is shown in Table 1.

The HEATING-6 results for Case-1 are presented in Figure 2 which shows isotherms in the crust at successive time periods illustrating the crust dynamic behavior, and in Figure 3 which shows isotherms in the shell itself. For the boundary conditions supplied for this case, a crust first grows to a maximum thickness of only about 1 cm (Fig. 2A) and then shrinks again to zero thickness (Fig. 2C). The shell quickly heats to 1000 K where it would be expected to fail due to lack of strength. Under the unrealistic assumption that it would stay in place, it further heats up to its melting temperature (assumed to be 1750 K). The melting interface is seen to move across the entire cross-section.

CASE-2:

Case-2 is a variation on Case-1 in which the melt depth was arbitrarily decreased to approximately two-thirds of the value of Case-1 to assess the effects of that parameter. The input crusting temperature was also reduced to 2050 K (this was not expected to have a significant impact on the results). The results are shown in Figure 4 which is a plot of the transient temperatures at various distances into the shell at the location of the maximum shell temperature. It is seen that, for the otherwise identical initial conditions, reducing the melt depth to this value is still not sufficient to prevent the prediction of temperatures at which the shell would be expected to fail.

Table 1. Heating-6 input values for cases 1-3

Transient input from CORCON		Input for both Cases 1 and 2	
Time (sec)[a]	Heat flux (W/m^2) melt-to-crust[b] ($\times 10^{-4}$)	Melt temperature (K)	Power density (W/m^3) decay + chem rx[c] ($\times 10^{-6}$)
0	18.3	2382	0.4
1	20.8	2379	22.1
31	75.5	2335	17.5
61	211.7	2352	15.5
91	376.6	2368	13.3
121	199.6	2339	7.7
151	144.9	2283	1.7
181	78.0	2216	0[d]
211	40.1	2163	0[d]
241	20.6	2121	0[d]
271	13.3	2089	0.16
301	10.4	2065	6.2
331	6.2	2043	0.3
361	5.1	2030	0.9
391	4.5	2021	0.9
421	3.8	2013	0.9
451	3.3	2006	0.9
481	2.8	1999	0.8
511	2.4	1993	0.8
541	2.1	1988	0.8
571	1.8	1983	0.8

Other Parameters

	Case 1	Case 2	Case 3
Melt-to-crust heat flux (W/M^2)	see above	see above	5×10^5
Melt temperature (K)	see above	see above	2150
Crusting temperature (K)	2150	2050	2100
Power density in crust (W/M^3)	see above	see above	1.07×10^5[e]
Debris depth (M) (vertical)	0.118	0.078	0.118
Crust thermal conductivity (W/M-K)	4.7	4.7	3.0 (UO_2)
Crust density	UO_2	UO_2	UO_2
Crust specific heat (J/g-K)	0.74	0.74	UO_2
Shell emissivity	0.3	0.3	0.7
Concrete emissivity	0.3	0.3	0.7

[a]Time = 0 sec at melt-shell contact.

[b]Computed from CORCON as $Q/A = h_{liq\ side}(T_{melt} - T_{solidus})$.

[c]Used only where HEATING-6 determines crust existence.

[d]CORCON computed endothermic reactions with energy absorption rates larger in magnitude than decay power. Power density input as 0.0 for conservatism.

[e]Decay power only.

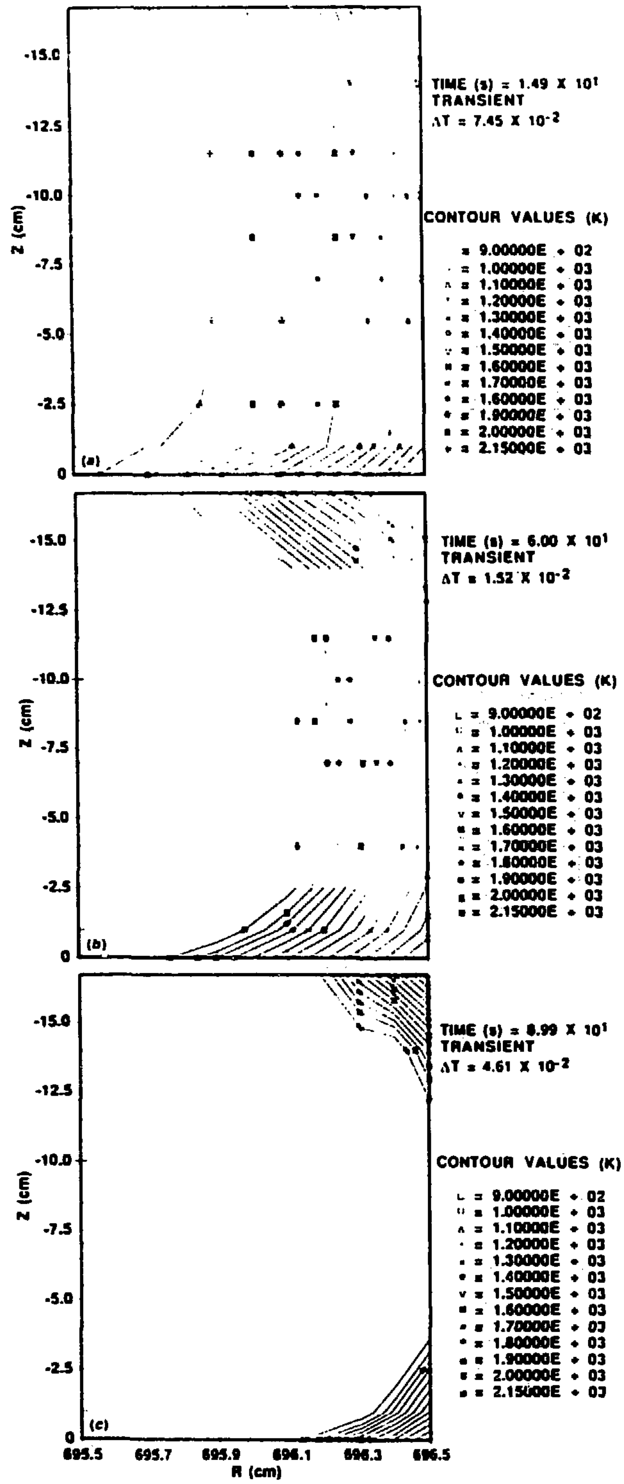

Fig. 2. Isotherms in crust at different times.

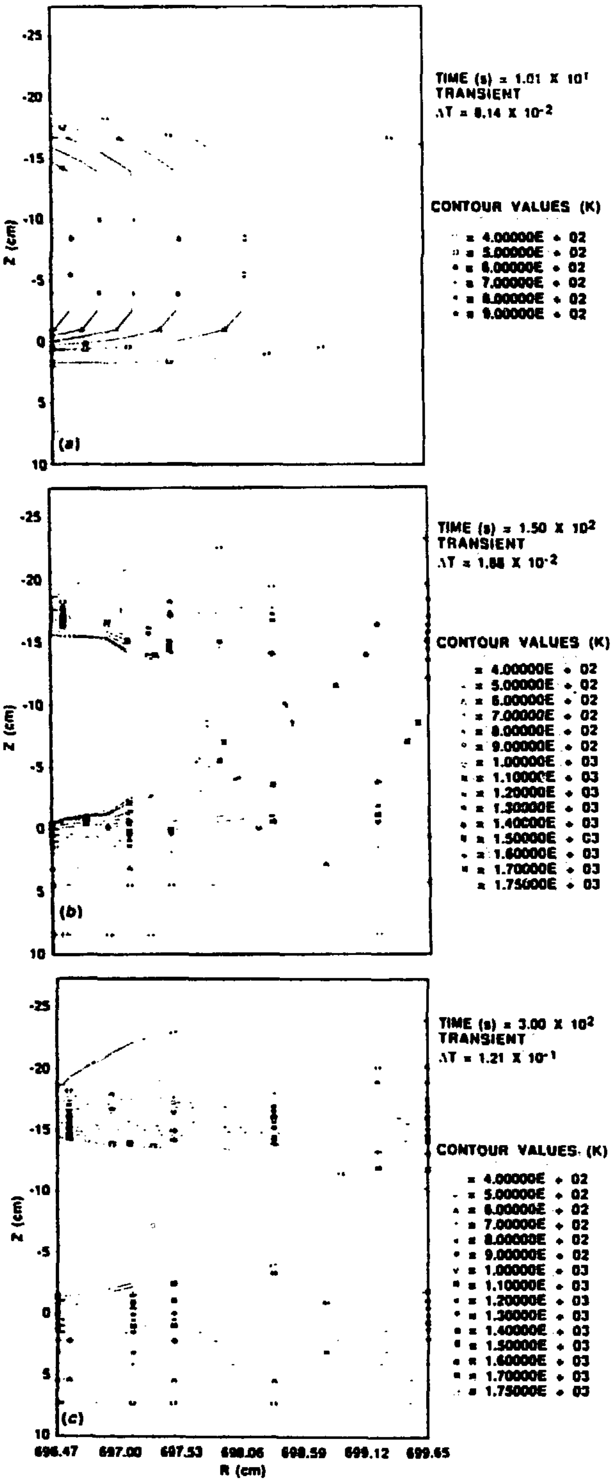

Fig. 3. Isotherms in containment shell at different times.

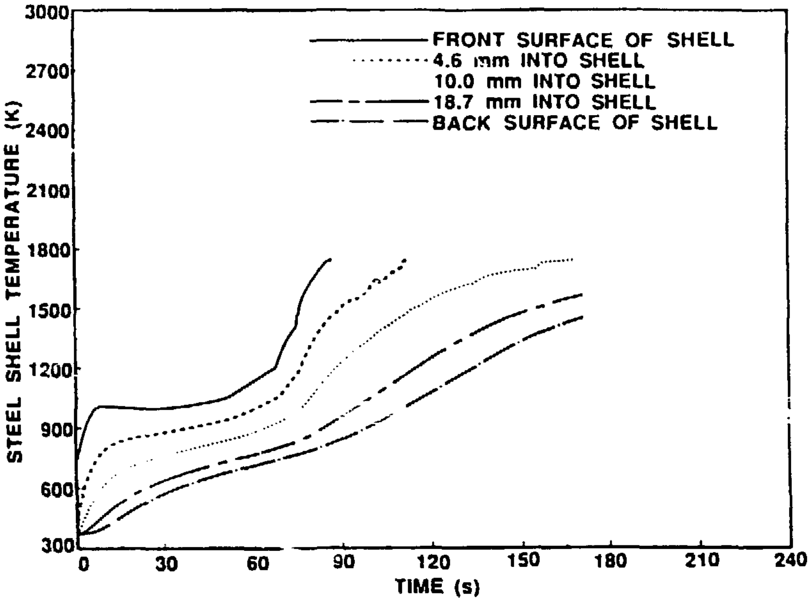

Fig. 4. Transient temperatures in containment shell (case 2).

CASE-3:

Case-3 is another variation of the base case performed in an attempt to investigate the effect of assumed parameters that are more favorable for the shell survival. The changes made to the base case for this variation included: The surface emissivities of the shell and of the concrete were increased from 0.3 to 0.7. The heat flux at the melt/crust interface was input at a constant value of 5×10^5 W/M^2 compared to the transient values for Case 1, some of which were above 2×10^6 W/M^2. The crust thermal conductivity was given the lower values representative of UO_2 (3.0 W/M-K) rather than the higher values (up to 6 W/M-K) given in CORCON for the melt mixture.

The results for this case are presented in Figure 5. It is seen that shell temperatures are still above the 1000 K level and are approaching melting after ~500 s.

CASE-4 and -5:

The development of the BWRLAP correlation was done in such a way as to allow it to be "benchmarked" to the HEATING-6 code through specification of the effectiveness factor (EF) previously discussed. Case-4 and -5 were run specifically for this purpose. Both cases were deliberately chosen to result in shell maximum temperatures that were below the melting value so as to be within the range of validity of the BWRLAP model. Case-4 assumed a high crusting temperature (2600 K) and a high melt-to-crust heat transfer coefficient of 10000 W/M^2-K, but used a low melt superheat (10 K) that would allow a very thick crust to develop (approximately 8 cm). Figure 6 presents the Heating-6 results compared with the prediction of BWRLAP for an EF of 0.85.

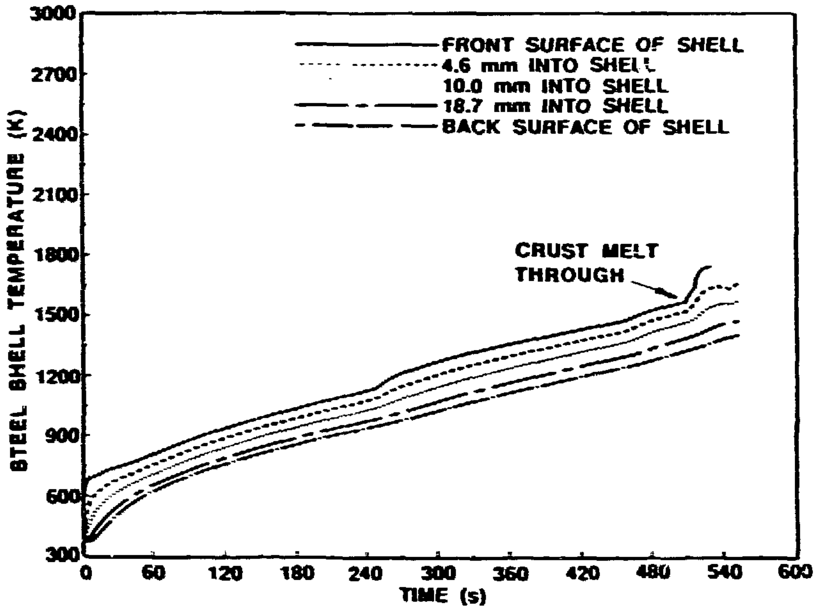

Fig. 5. Transient temperatures in containment shell (case 3).

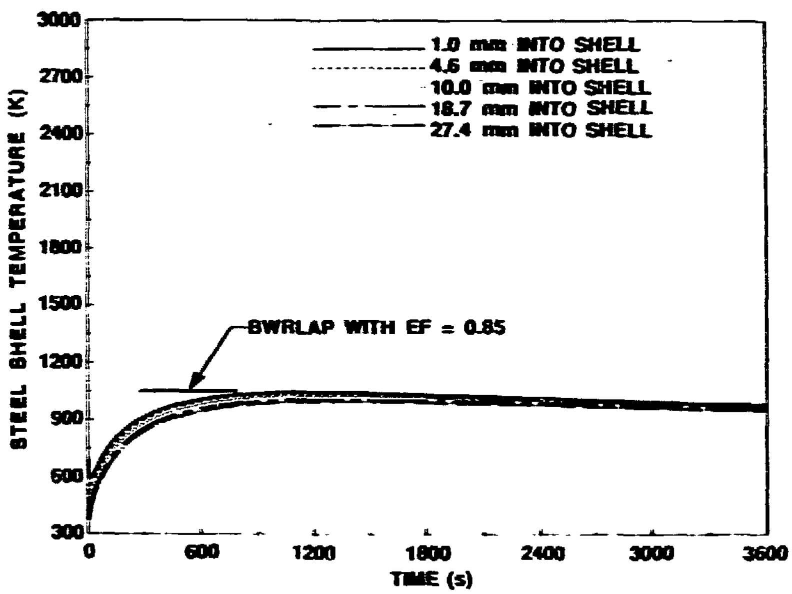

Fig. 6. Transient temperatures in containment shell (case 4).

Case-5 assumed a lower crusting temperature (2100 K), a lower heat transfer coefficient (5000 W/M²-K), but a larger melt superheat (50 K) resulting in a much thinner crust (approximately 1 to 2 cm) thereby providing a significant "stressing" range for the BWRLAP correlation. The results compared with the BWRLAF calculation for the same EF of 0.85 are shown on Figure 7. It is seen in Figures 6 and 7 that the BWRLAP model compares well with HEATING-6 (this is true for both the maximum liner temperature and for the crust thickness). This provides confidence in the BWRLAP correlation as being reasonably representative of the important features of the problem.

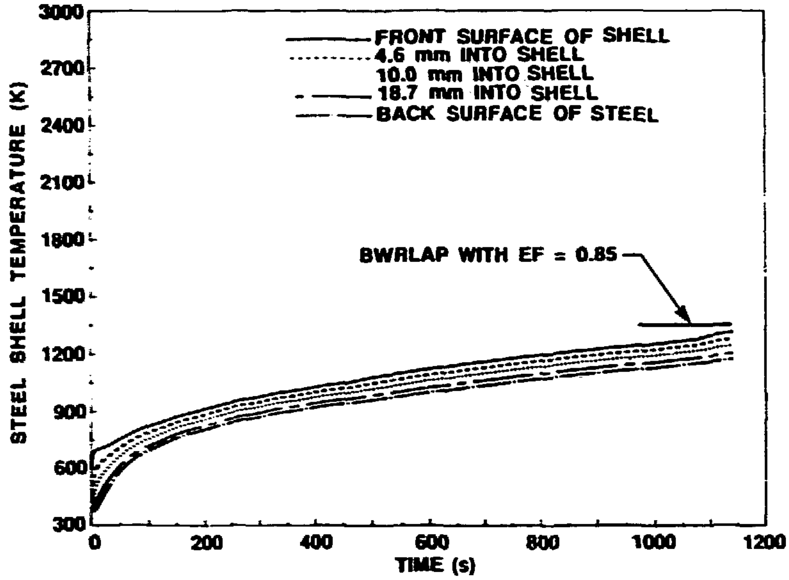

Fig. 7. Transient temperatures in containment shell (case 5).

BWRLAP Parametric Study

Both HEATING-6 and BWRLAP require (in one form or another) input of the following parameters the values of which are believed to be highly uncertain: the crusting temperature, the superheat, the melt depth, and the melt-to-crust heat transfer coefficient. To determine the sensitivity of the results to these inputs, calculations were made with BWRLAP for the following parameter values:

- crusting temperature (K) .... 1800; 2200; 2600.
- melt depth (cm) .... 5; 10; 15; 20.
- heat transfer coefficient (W/M²-K) 5000; 10000
- superheat (K) .... [varied systematically until the shell melt temperature (1750 K) was reached].

The results of the parameter study are presented in Figure 8 (for h = 10000) and Figure 9 (for h = 5000). It can be seen from these figures that the shell maximum temperature is relatively insensitive to the absolute level of the crusting temperature (and therefore the melt temperature) but is very sensitive to the superheat (the difference between the melt temperature and the crusting temperature) especially for melt depths of 10 cm or greater where the curves are very steep. There is moderate sensitivity to the melt-to-crust heat transfer coefficient. Reducing the value from 10000 to 5000 W/M^2-K basically allows the superheat to double for a given shell maximum temperature. This is better illustrated on Figure 10 which presents the maximum superheat values allowed before the liner maximum temperature exceeds 1000 K (failure) as a function of melt depth for two values for the melt-to-crust heat transfer coefficient (10000 and 5000 W/M^2-K).

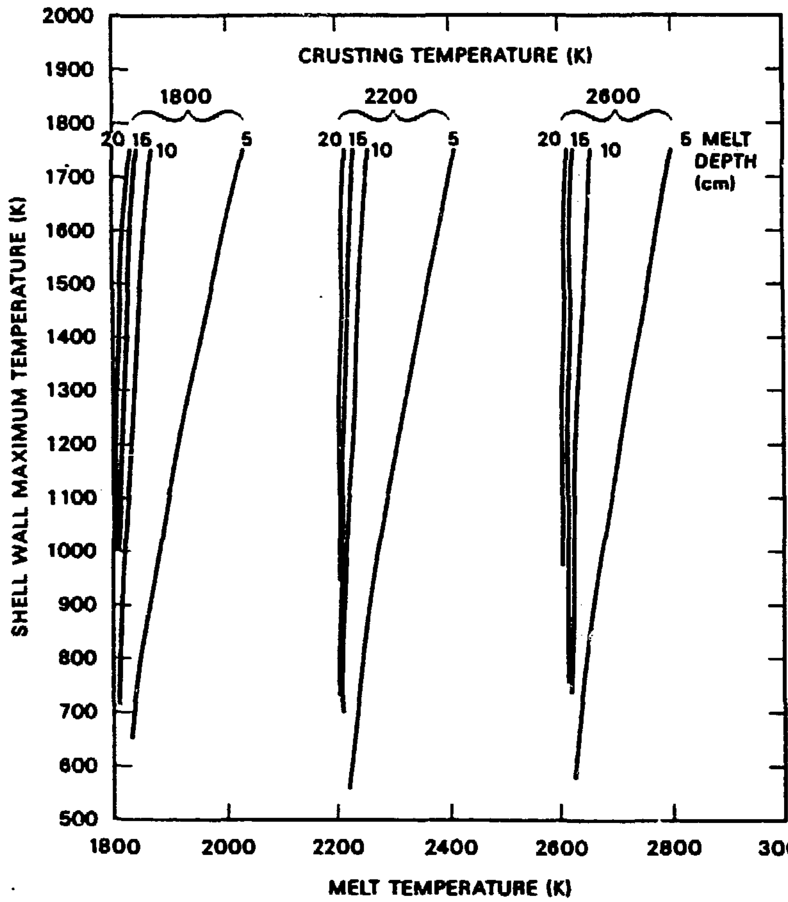

Fig. 8. Maximum shell temperature vs melt temperature as a function of crusting temperature and melt depth for a melt convective heat transfer coefficient of 10,000 (W/M^2-K).

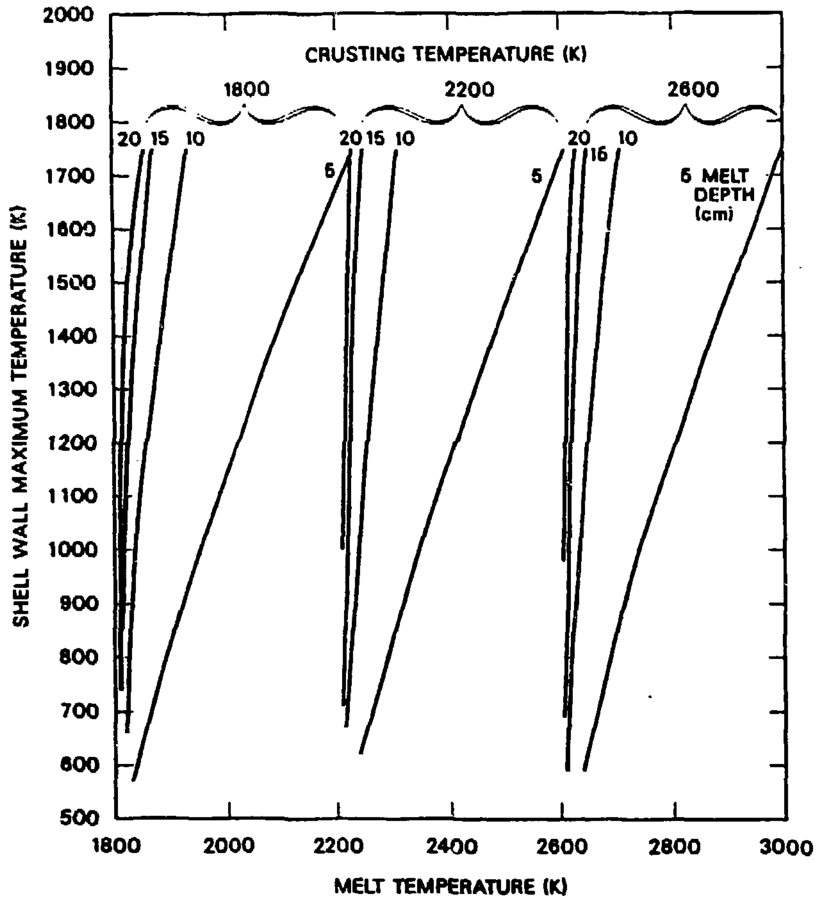

Fig. 9. Maximum shell temperature vs melt temperature as a function of crusting temperature and melt depth for a melt convective heat transfer coefficient of 5,000 ($W/M^2/K$).

Figure 11 shows the calculated values for the crust thicknesses as a function of the superheat for a crusting temperature of 2600 K and for the two values for the heat transfer coefficient. As would be expected, the crust thickness gets very large at small superheats and small at large superheats. This result is not very sensitive to the actual crusting temperature.

The sensitivity of the results to the thickness of the shell itself can easily be addressed by the BWRLAP correlation. Table 2 compares the results for shell thicknesses of 2.16 cm and 3.18 cm. Moderate sensitivity to this parameter is noted in that at a melt depth of 10 cm, the 32% reduction in thickness resulted in a 25% reduction in the limiting superheat before melting temperature was exceeded.

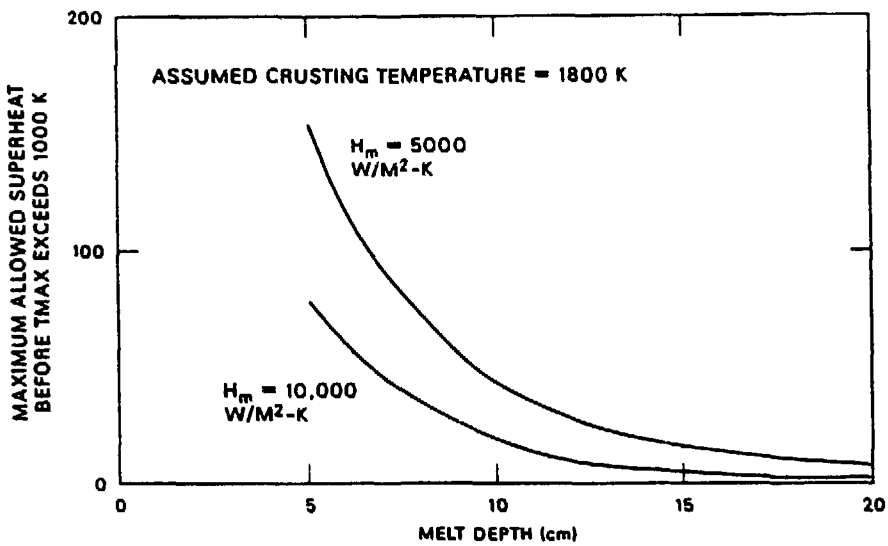

Fig. 10. Superheat (melt temperature – crusting temperature) above which th shell maximum temperature exceeds 1,000 K as a function of the melt depth and the melt-to-crust heat transfer coefficient.

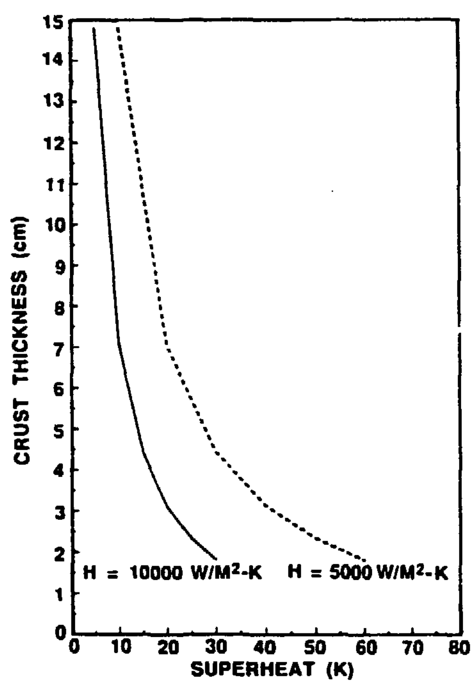

Fig. 11. Crust thickness vs superheat (melt temperature – crusting temperature), for a crusting temperature of 2,600 K, melt-to-crust heat transfer coefficients of 10,000 and 5,000 (W/M²-K), and melt depth of 15 cm.

Table 2. Superheat required to produce shell maximum temperature of 1750 K for the indicated shell thickness

Melt depth (cm)	Superheat (K) for shell thickness (cm)	
	3.18	2.16
5	235	170
10	75	55
15	40	33
20	31	27

CONCLUSIONS

This study provides a clear understanding of the dominant parameters that influence the thermal response of the BWR MARK-I containment shell upon contact with molten core materials. The important parameters are:

- melt superheat.
- melt depth.
- melt-to-crust heat transfer coefficient.

These parameters are generally determined by computer codes that treat the melt progression (MP) and molten-core/concrete interaction (MCCI) phases of a severe accident. These required inputs from the MP and MCCI codes are believed to be subject to much uncertainty, particularly with respect to the melt spreading behavior and the effects of existing water within the reactor cavity. Without a clearer understanding of these uncertainties and their quantification, it is not possible to provide an unqualified resolution to this issue at this time. The HEATING-6 model is now available and can provide a credible evaluation of the containment shell thermal response when new and less uncertain contact boundary conditions become available.

REFERENCES

1. G. A. Greene, K. R. Perkins, and S. A. Hodge, "Mark I Containment Drywell: Impact of Core-Concrete Interactions on Containment Integrity and Failure of the Drywell Liner," Proceedings of the International Symposium on Source Term Evaluation for Accident Conditions, IAEA (October 1985).

2. D. C. Elrod, G. E. Giles, and W. D. Turner, "HEATING-6, A Multidimensional Heat Conduction Analysis with Finite Difference Formulation. In Scale, A Modular Code System for Performing Standardized Computer Analyses for Licensing Evaluations," NUREG/CR-0200, ORNL/NUREG/CSD-2/R1.

3. C. B. Byran, K. W. Childs, G. E. Giles, "HEATING-6 Verification," K/CSD/TM-61, December 1986.

4. K. W. Childs, C. B. Byran, "HEATING-6 Analysis of International Thermal Benchmark Problem Sets 1 and 2," ORNL/CSD/TM-239, October 1986.

5. C. B. Byran and K. W. Childs, "Thermal Codes Benchmarking – HEATING-6 Results," K/CSD/TM-57, August 1985.

APPENDIX I

DESCRIPTION AND DERIVATION OF THE BWRLAP CORRELATION

The objective of the BWR Liner Analysis Program (BWRLAP) is to correlate the steady-state temperature distribution in a BWR MARK-I containment steel shell when contacted by molten core materials. The shell is assumed to be cooled by water overlying the melt and by radiative and convective heat transfer off its back side to surrounding concrete. A crust is assumed to have formed between the shell and the melt of a thickness to be determined by the solution of the problem itself.

Derivation of the governing equations:

Refer to the geometric representation of the BWRLAP model shown below for the derivation that follows.

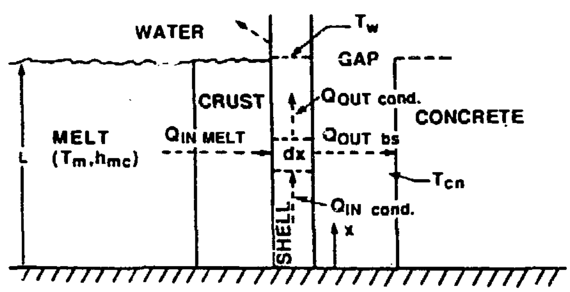

The derivation of the BWRLAP model is based on the following implied assumptions:

- The temperature gradient across the shell (in the R-direction) is small enough to be neglected.
- The cooling of the shell in its region of contact with the water overlying the melt is so effective that a low value (near the water temperature) can be assumed for the temperature at that interface.
- The rate of heat-up of the concrete surrounding the backside of the shell is slow compared to the initial response of the shell so that a quasi-steady state solution is sufficient and the concrete temperature can be assumed to have small effect on the radiative losses from the back side of the shell.
- The heat transfer from the melt to the crust is given by the product of a heat transfer coefficient h_m and the difference between the melt temperature T_m and the crusting temperature T_c, all of which are assumed constant in this model. The portions of this heat that are lost to the

overlying water and to the underlying floor are represented in the correlation by utilizing an "effectiveness factor" (EF) to decrease the heat transfer calculated by a series conduction-like fin equation that must be calibrated to a known solution.

A heat balance at any vertical axial location, x, in the shell can be made as follows:

$$Q_{in\ cond} + Q_{in\ melt} = Q_{out\ bs} + Q_{out\ cond} \cdot$$

The relationships used for the above heat flow quantities are given below:

$$Q_{in\ cond} = -k\ A_{cs}\ (dT/dx)$$

$$Q_{out\ cond} = -k\ A_{cs}\ [dT/dx + (d^2T/dx^2)(dx)]$$

$$Q_{in\ melt} = h_{eff}\ A_p\ (T_m - T)$$

$$Q_{out\ bs} = h_{bs}\ A_p\ (T - T_{cn})$$

where

$$h_{eff} = [1/h_{mc}\ +\ Th_c/k_c]$$

$$h_{bs} = h_{nc} + h_r$$

h_{mc} = The melt-to-crust convective heat transfer coefficient.

Th_c = The crust thickness in the R-direction.

k_c = The crust thermal conductivity.

h_{nc} = The natural convection heat transfer coefficient in the air gap behind the shell.

h_r = An "effective" radiation heat transfer coefficient between the shell and the concrete (to be discussed later).

k = The shell thermal conductivity.

A_{cs} = The cross-sectional area of the shell per unit circumferential distance.

A_p = The surface area of element dx for unit circumferential distance.

T = The shell temperature.

T_m = The melt temperature.

T_{cn} = The temperature of the concrete behind the shell.

It is noted here that the use of h_{eff} is not the normal series conduction concept. In the BWRLAP correlation it is used as a convenient means to account for the heat losses from the crust top and bottom surfaces. The implied assumption is that these losses are essentially proportional to the crust thickness. Substituting the above into the heat balance equation gives:

$$kA_{cs}(d^2T/dx^2) + h_{eff}(T_m - T) - h_{bs}(T - T_c) = 0 \ . \qquad \text{(Eq. I-1)}$$

Note that, for zero crust thickness, the above reduces to the exact "fin" equation with a heat source on one side and a heat sink on the other.

Defining T' as $(T_m - T)$, Eq. I-1 becomes

$$d^2T'/dx^2 - A\,T' = B \ , \qquad \text{(Eq. I-2)}$$

where

$A = (h_{eff} + h_{bs})/(kt_w)$

$B = -(h_{bs})(T_m - T_{cn})/(kt_w)$

t_w = shell wall thickness

and the boundary conditions are

at $x = 0$; $dT'/dx = 0$,

at $x = L$; $T' = (T_m - T_w)$.

In these boundary conditions, T_w is the temperature of the wall at the location of its interface with the water coolant. It is presumed that this can be arbitrarily specified to be a low value near the water temperature itself. The distance "L", while nominally considered to be the "slant depth" or contact length of the melt with the shell is left here as an unspecified length less than this value. This allows "benchmarking" the BWRLAP correlation to the more exact 2-D analysis of HEATING-6 that accounts for the heat losses to the water as well as for heat to be transferred downward through the shell into the concrete below the floor. This "benchmarking" will also allow folding in the effects of using a convective-like equation to model radiation heat transfer off the side of the shell facing the concrete.

The homogeneous solution to Eq. I-2 is

$$T' = C_1 \exp(A^{1/2}x) + C_2 \exp(-A^{1/2}x) \ .$$

A particular solution is

$$T' = -B/A \ .$$

Therefore, the full general solution is

$$T' = C_1 \exp(A^{1/2}x) + C_2 \exp(-A^{1/2}x) - B/A \ .$$

Applying the boundary conditions, this becomes

$$T' = \frac{(T_m - T_w + B/A)}{[\exp(A^{1/2}L) + \exp(-A^{1/2}L)]} [\exp(A^{1/2}x) + \exp(-A^{1/2})] - B/A \qquad \text{(Eq. I-3)}$$

The maximum temperature in the shell will occur at the location of $x = 0$. The value of T' at this location (designated T'_{max}) is given by

$$T'_{max} = (2)\ (T_m - T_w + B/A)/[\exp(A^{1/2}L) + \exp(-A^{1/2}L)] - B/A \ . \qquad \text{(Eq. I-4)}$$

The maximum shell temperature itself, from our definition of T', is

$$T_{max} = T_m - T'_{max} \ .$$

Equations I-3 and I-4 form the fundamental basis of the BWRLAP correlation. In the BWRLAP application, the melt depth is divided by an "effectiveness factor" (EF) to correct for the slant height (cos 45°), to account for heat losses from the top and bottom of the crust, and to account for the 2-D shunting effects of the crust. However, these do not yet represent a completely closed solution because we have left unspecified the exact crust thickness. In addition, the back-side radiation heat transfer is a function of the fourth power of the as yet undetermined liner temperature distribution. Consequently, the above equations were programmed into a PC and an iterative procedure was used to establish both the crust thickness, Th_c, and the back-side heat transfer coefficient, h_{bs}.

<u>Procedure for determining crust thickness and the back-side equivalent radiative heat transfer coefficient</u>

The crust thickness is determined by an iterative procedure that balances the heat going from the melt into the EF corrected melt/crust interface with the heat going from the interface to the shell itself. Recall that this EF reduces the magnitude of the heat to the shell as a way of accounting for losses at the crust upper and lower surfaces.

The heat (per unit circumferential distance) going from the melt into the melt/crust interface is given by

$$Q_{mc} = h_{mc}L(T_m - T_c) \quad \text{(Eq. I-5)}$$

where T_c = the crusting temperature of the melt.

The heat (per unit circumferential distance) going from the crust interface into the shell is given by

$$Q_1 = \int_0^{L/EF} (k_c/Th_c)\ (T_c - T)dx \quad \text{(Eq. I-6)}$$

The following algorithm is used:

- An arbitrary crust thickness is assumed.
- An arbitrary h_{bs} is assumed.
- Equation I-3 is solved for the temperature distribution in the shell.
- Equation I-6 is integrated for this temperature distribution to obtain Q_1.
- The crust thickness is iterated upon until Q_{mc} (Eq. I-5) equals Q_1 (Eq. I-6).
- A second level iteration is then made on h_{bs} as discussed below until convergence is achieved for both Th_c and h_{bs}.

The heat transfer from the back-side of the shell to the concrete is considered to be by both radiation and natural convection. BWRLAP uses an effective convective relationship for this,

$$Q_{bs} = (h_{nc} + h_{rad})\ (T - T_{cn})\ .$$

Preliminary calculations have indicated that the radiation contribution dominates over the natural convection. Therefore, a constant representative value is input for h_{nc}. The effective radiation coefficient is calculated internally by the relationship

$$h_{rad} = [C/(1/e_1 + 1/e_{cn} - 1)][1/L \int_0^L (T^3 + T^2T_{cn} + TT_{cn}^2 + Tcn^3)dx]\ .$$

This "averaging" assures that the radiation heat transfer off the back side has the correct total amount but distributes it differently along the shell length. This is not considered to introduce a serious error in the determination of the maximum shell temperature.